Surface Ionization State and Nanoscale Chemical Composition of UV-Irradiated Poly(dimethylsiloxane) Probed by Chemical Force Microscopy, Force Titration, and Electrokinetic Measure...

ARTICLE *in* LANGMUIR · JUNE 2007

Impact Factor: 4.46 · DOI: 10.1021/la063168s · Source: PubMed

7 AUTHORS, INCLUDING:

Jing Song
Agency for Science, Technology and Researc...
35 PUBLICATIONS **418** CITATIONS
SEE PROFILE

Martien Cohen Stuart
Wageningen University
176 PUBLICATIONS **5,314** CITATIONS
SEE PROFILE

H. Hillborg
ABB
59 PUBLICATIONS **1,657** CITATIONS
SEE PROFILE

Gyula Julius Vancso
University of Twente
277 PUBLICATIONS **6,481** CITATIONS
SEE PROFILE

Surface Ionization State and Nanoscale Chemical Composition of UV-Irradiated Poly(dimethylsiloxane) Probed by Chemical Force Microscopy, Force Titration, and Electrokinetic Measurements

Jing Song,[†] Jérôme F. L. Duval,[‡] Martien A. Cohen Stuart,[§] Henrik Hillborg,[†,||] Ullrich Gunst,[⊥] Heinrich F. Arlinghaus,[⊥] and G. Julius Vancso*[,†]

Dutch Polymer Institute and MESA+ Institute for Nanotechnology, Materials Science and Technology of Polymers, University of Twente, P.O. Box 217, 7500 AE Enschede, The Netherlands, Laboratory Environment and Mineral Processing, Nancy-University, CNRS, Research Center Francois Fiessinger, 15 Avenue du Charmois, BP40, 54501 Vandoeuvre-lès-Nancy cedex, France, Laboratory of Physical Chemistry and Colloid Science, Wageningen University, P.O. Box 8038, 6700 EK Wageningen, The Netherlands, ABB AB, Corporate Research, Power Technology, Västerås SE 72178, Sweden, and Physikalisches Institut, Wilhelm-Klemm-Str. 10, Westfälische Wilhelms-Universität, D-48149 Münster, Germany

Received October 30, 2006. In Final Form: February 9, 2007

The surface chemistry and ionization state of cross-linked poly(dimethylsiloxane) (PDMS) exposed to UV/ozone were studied as a function of treatment time. Various complementary and independent experimental techniques were utilized, which yielded information on the macroscopic as well as the nanometric scale. The average chemical composition of the PDMS surface was quantitatively investigated by time-of-flight secondary ion mass spectrometry (ToF-SIMS). It was found that the top 1−2 nm surface layer was dominated by silanol groups (−SiOH) for which the concentration increased with increasing treatment dose. The lateral distributions of the silanol groups were analyzed on the nanometer scale by means of atomic force microscopy (AFM) with chemically functionalized tip probes in aqueous buffer solutions at varying pHs. Spatially dependent pull-off force curves (also called "force volume" imaging) indicated the presence of strong chemical heterogeneity of the probed surface. This heterogeneity took the form of patches of silanol functionalities with high local concentration surrounded by a matrix of predominantly hydrophobic domains at low pH. The average pull-off forces for the entire surface scanned were significantly reduced for pH values larger than a characteristic pK_a constant (in the range between 4.5 and 5.5). The extent of the decrease in the pull-off force and the particular value of pK_a were found to be a function of treatment time and to differ from the commonly reported values for silanol functional groups on a homogeneous silica surface. These dependences were ascribed to the evoking of a protonation/deprotonation process of the surface silanol groups which was sensitive to the hydrophobic/hydrophilic balance of their close molecular environment. Intermolecular hydrogen bonding may also account for the shifts in the surface pK_a. Furthermore, depending on the nature of the electrolyte, a third effect related to double layer composition, as determined by specific ion adsorption, was quantitatively analyzed by streaming potential measurements in the presence of sodium chloride and phosphate electrolytes.

Introduction

Poly(dimethylsiloxane) (PDMS) is a unique polymer with a variety of intriguing properties related to the chemical structure of its Si−O backbone and substitution on Si.[1] Cross-linked PDMS elastomers are widely used as insulating and protective materials in both high- and low-temperature rubber applications, in soft lithography as stamps for microcontact printing, and in the microfabrication of micro-electro-mechanical system (MEMS) devices.[2−7] However, despite the very useful bulk properties, including a modulus which does not vary significantly over a broad temperature range, selective gas permeability,[8] and long-term endurance, the low surface tension of PDMS limits its use in surface-related applications.

Reduction of the hydrophobicity can be achieved by exposing PDMS to various types of oxidizing plasmas, corona discharges, or UV radiation.[9−12] Such surface treatments have been adopted for controlling the wettability and to render the PDMS surface more hydrophilic. For instance, in microfluidic applications, a decrease in the hydrophobicity of PDMS improves the wettability of aqueous solutions and leads to the reduction of air bubble nucleation in the microchannels.[13] To properly adjust the surface characteristics of PDMS for the aforementioned applications, it

* To whom correspondence should be addressed. E-mail: g.j.vancso@tnw.utwente.nl.
[†] University of Twente.
[‡] Nancy-University.
[§] Wageningen University.
[||] ABB AB.
[⊥] Westfälische Wilhelms-Universität.

(1) Brook, M. A. *Silicon in Organic, Organometallic, and Polymer Chemistry*; John Wiley & Sons: New York, 2000.
(2) Xia, Y. N.; Whitesides, G. M. *Annu. Rev. Mater. Sci.* **1998**, *28*, 153.
(3) Kane, R. S.; Takayama, S.; Ostuni, E.; Ingber, D. E.; Whitesides, G. M. *Biomaterials* **1999**, *20*, 2363.
(4) Lahiri, J.; Ostuni, E.; Whitesides, G. M. *Langmuir* **1999**, *15*, 2055.
(5) Degenhart, G. H.; Dordi, B.; Schönherr, H.; Vancso, G. J. *Langmuir* **2004**, *20*, 6216.
(6) Hillborg, H.; Gedde, U. W. *IEEE Trans. Dielectr. Electr. Insul.* **1999**, *6*, 703.
(7) Hall, J. F. *IEEE Trans. Power Delivery* **1993**, *8*, 376.
(8) Merkel, T. C.; Bondar, V. I.; Nagai, K.; Freeman, B. D.; Pinnau, I. *J. Polym. Sci., Part B: Polym. Phys.* **2000**, *38*, 415.
(9) Efimenko, K.; Wallace, W. E.; Genzer, J. *J. Colloid Interface Sci.* **2002**, *254*, 306.
(10) Fateh-Alavi, K.; Gedde, U. W. *Polym. Degrad. Stab.* **2004**, *84*, 469.
(11) Kind, H.; Bonard, J. M.; Emmenegger, C.; Nilsson, L. O.; Hernadi, K.; Maillard-Schaller, E.; Schlapbach, L.; Forro, L.; Kern, K. *Adv. Mater.* **1999**, *11*, 1285.
(12) Berdichevsky, Y.; Khandurina, J.; Guttman, A.; Lo, Y. H. *Sens. Actuators, B* **2004**, *97*, 402.
(13) Martin, B. D.; Brandow, S. L.; Dressick, W. J.; Schull, T. L. *Langmuir* **2000**, *16*, 9944.

10.1021/la063168s CCC: $37.00
Published on Web 04/07/2007

is critical to understand the changes that the PDMS surface undergoes when exposed to various surface treatments.

It has been shown that, during treatment-dependent surface modifications of PDMS, silanol groups are introduced at the surface.[14] Recently, Graubner et al. thoroughly investigated the mechanism of photochemical alteration of PDMS.[15] They concluded that the photochemical conversion of surface methylsilane groups to silanol groups is responsible for the large increase in surface free energy. Oxidative cross-linking via Si−O bridges was found to cause the gradual formation of a continuous "silica-like" barrier layer of SiO_2. The oxidation process within the top 10 nm of the surface has been extensively investigated by X-ray photoelectron spectroscopy (XPS), proving the existence of this silica-like layer.[14−18] To gain further understanding of the oxidizing processes, it is important to elucidate the development of lateral heterogeneities in the surface chemistry on a submicrometer scale as a function of treatment time.

Compared to other vacuum-based surface characterization techniques such as XPS and scanning electron microscopy (SEM), atomic force microscopy (AFM) can be utilized with surface functionalized tips and is in this case often referred to as chemical force microscopy (CFM). This technique exhibits the advantage that measurements can be carried out in solvents and salt solutions (electrolytes).[19,20] CFM thus combines the high spatial resolution of AFM with further chemical discrimination as introduced by chemically functionalized scanning probe tips that, upon approach, locally interact with the surface to be analyzed.

The subject of mapping the surface hydrophobicity of UV/ozone-treated PDMS as a function of storage time by CFM has already been addressed in one of our earlier studies.[21] However, the coverage and surface distribution of the functional groups as well as the ionic state introduced during their oxidization process have received little attention. In this paper, UV/ozone irradiation was used to mimic the oxidation process since the resulting chemical changes were similar to those introduced by the fast (and therefore less controlled) oxygen plasma techniques.[22−24] The interaction forces (adherence) between the chemically modified tip and the PDMS surface were measured by CFM and were found to be highly sensitive to the changes in the ionization state of the terminal surface functionalities as induced by varying the solution composition (pH, ionic strength) and the surface treatment time. Force titration curves, monitoring the tip−sample adherence as a function of pH, were used to determine and map the pK_a of the functional surface groups at a ∼20 nm resolution.[25]

To gain further insights into the molecular origins of the pK_a shifts when varying the electrolyte composition and/or UV/ozone exposure time, the knowledge of the overall surface ionization state (macroscopic scale) was also essential. Therefore, UV/ozone-treated PDMS surfaces were further investigated by streaming potential measurements in various electrolytes of which the ion concentrations were varied. A critical examination of the variations in the so-determined isoelectric points (IEP)[26−28] with surface treatment and electrolyte composition was performed. Hence, it was possible to address the role played by the specific ionic interaction in the determination of the effective surface pK_a. The measured streaming potentials were quantitatively interpreted on the basis of a double layer model that coupled the classical Gouy−Stern scheme with the site dissociation theory.[29] The combination of the nano- and macroscale analyses of the PDMS surface leads to the identification of the physicochemical processes that affect the effective pK_a of the PDMS surface, namely the presence of hydrophobic nanometer-sized domains stabilized by UV/ozone irradiation, the formation of lateral hydrogen bonding, and specific ion adsorption phenomena.

Materials and Methods

PDMS Film Preparation. All experiments were performed using an elastomeric PDMS kit manufactured by Dow Corning. Sylgard-184A (elastomer) and Sylgard-184B (curing agent) were used without modification and mixed at a mass ratio of 10:1. Glass cover slides were cleaned using a Piranha solution (1:4 mixture of 30% H_2O_2 and concentrated H_2SO_4), carefully rinsed several times in Milli-Q water and ethanol, and finally dried in a stream of nitrogen gas. ***Caution!*** *Piranha solution is a very strong oxidant, which reacts violently with organic materials and should therefore be handled with the utmost care!* The PDMS was then spin coated onto the cleaned glass substrates using a spin coater model P6700 (Specialty Coating Systems, Inc). The film thickness was 800 nm ± 100 nm according to the ellipsometry measurements (Plasmos SD 2002 ellipsometer). After spin coating, the films were cured overnight at 120 °C and then stored individually in plastic containers at ambient temperature.

UV/Ozone Treatment. UV/ozone treatment of the PDMS surface was carried out in a commercially available UV/ozone chamber (Ultra-Violet Products PR-100). A typical treatment chamber contains a low-pressure mercury UV light, generating UV emissions at 185 nm (1.5 mW cm^{-2}) and 254 nm (15 mW cm^{-2}). The distance between the UV source and the PDMS films was 20 mm for the particular setup used in this study. A nominal steady-state concentration of ozone at 55 ppm was produced in a two-step photochemical process initiated by the photolysis of molecular oxygen at 185 nm. The 254 nm radiation can be absorbed by most hydrocarbons, as well as by ozone. The organic samples reacted with atomic oxygen to form simpler, volatile molecules, which desorbed from the surface.

Since the surface energy of the UV/ozone-treated PDMS was a function of storage time,[21] all the following characteristic measurements were performed directly after the treatment.

AFM Tip Modification. Triangular shaped silicon nitride cantilevers and silicon nitride tips (Veeco Digital Instruments (DI), Santa Barbara, CA, U.S.A.) coated with ∼2 nm Ti as the adhesion layer and ∼50 nm Au in high vacuum were used in the AFM experiments. The functional groups at the tip surface were introduced by self-assembled monolayers (SAMs). The tips were prepared by immersion in a 1 mM 11-mercapto-1-undecanol solution, with ethanol as the solvent, for 10−40 h at room temperature. The functionalized tips were kept in solution between measurements and then rinsed in ethanol and dried in a stream of nitrogen immediately before use. The spring constants of the cantilevers ranged from 0.14 to 0.28 nN nm^{-1}, as obtained by the method of Hutter and Bechhoefer.[30]

Chemical Force Microscopy (CFM). CFM was carried out with a NanoScope III multimode AFM (DI). A hydroxyl-terminated tip

(14) Hillborg, H.; Sandelin, M.; Gedde, U. W. *Polymer* **2001**, *42*, 7349.
(15) Graubner, V. M.; Jordan, R.; Nuyken, O.; Schnyder, B.; Lippert, T.; Kotz, R.; Wokaun, A. *Macromolecules* **2004**, *37*, 5936.
(16) Toth, A.; Bertoti, I.; Blazso, M.; Banhegyi, G.; Bognar, A.; Szaplonczay, P. *J. Appl. Polym. Sci.* **1994**, *52*, 1293.
(17) Owen, M. J.; Smith, P. J. *J. Adhes. Sci. Technol.* **1994**, *8*, 1063.
(18) Hillborg, H.; Gedde, U. W. *Polymer* **1998**, *39*, 1991.
(19) Frisbie, C. D.; Rozsnyai, L. F.; Noy, A.; Wrighton, M. S.; Lieber, C. M. *Science* **1994**, *265*, 2071.
(20) Noy, A.; Frisbie, C. D.; Rozsnyai, L. F.; *J. Am. Chem. Soc*. **1995**, *117*, 7943.
(21) Hillborg, H.; Tomczak, N.; Olah, A.; Schönherr, H.; Vancso, G. J. *Langmuir* **2004**, *20*, 785.
(22) Vasilets, V. N.; Nakamura, K.; Uyama, Y.; Ogata, S.; Ikada, Y. *Polymer* **1998**, *39*, 2875.
(23) Huck, W. T. S.; Bowden, N.; Onck, P.; Pardoen, T.; Hutchinson, J. W.; Whitesides, G. M. *Langmuir* **2000**, *16*, 3497.
(24) Ouyang, M.; Yuan, C.; Muisener, R. J.; Boulares, A.; Koberstein, J. T. *Chem. Mater.* **2000**, *12*, 1591.
(25) Schönherr, H.; Hruska, Z.; Vancso, G. J. *Macromolecules* **2000**, *33*, 4532.
(26) Duval, Y.; Mielczarski, J. A.; Pokrovsky, O. S.; Mielczarski, E.; Ehrhardt, J. J. *J. Phys. Chem. B* **2002**, *106*, 2937.
(27) Kim, K. J.; Fane, A. G.; Nyström, M. *J. Membr. Sci.* **1997**, *134*, 1999.
(28) Franks, G. V.; Meagher, L. *Colloids Surf., A* **2003**, *214*, 99.
(29) Yates, D. E.; Levine, S.; Healy, T. W. *J. Chem. Soc., Faraday Trans. 1* **1974**, *70*, 1807.
(30) Hutter, J. L.; Bechhoefer, J. *Rev. Sci. Instrum.* **1993**, *64*, 1868.

was brought into contact with a modified substrate and then retracted. For laterally resolved pull-off force measurements, the AFM was operated in the so-called force volume (FV) mode[31] using a 10 μm $\times$ 10 μm $x-y$-range scanner. Arrays of 64 $\times$ 64 points (corresponding to 4096 consecutive force measurements (force−distance curves)) were acquired on scan areas of 500 nm $\times$ 500 nm. Cycles of tip approach, contact, and retraction were recorded at a rate of 4 Hz with a vertical (Z) scan size on the order of 500 nm. The photodiode signal data and piezo displacement curves were transformed into force−distance data using a custom built Labview application.[21,32] Histograms of adherence were obtained.

This approach−contact−retract cycle was performed as a function of the solution pH. The most probable force of rupture versus pH, as derived from the aforementioned histograms, was referred to as the chemical force titration curve. All the force−distance curves were obtained in a liquid cell filled with buffer solution. The cell was thoroughly cleaned and then rinsed with ethanol and water prior to use. The buffer solution was freshly prepared using a phosphate salt (H_3PO_4, NaH_2PO_4, Na_2HPO_4) and kept at a constant ionic strength of 300 mM and at a pH ranging from 2 to 8. The measurements were carried out after an equilibration period of at least 1 h to minimize any instrument drift. More importantly, the pull-off force data did not change over time, indicating that the surface was in equilibrium with the buffer. For FV imaging, only subsequent up and down scans that showed the same force characteristics were considered. After the experiments, the tip radii were characterized by scanning an array of sharp spikes, resulting in so-called tip imaging. No obvious tip apex enlargement was observed.

Time-of-Flight Secondary Ion Mass Spectrometry (ToF-SIMS). In ToF-SIMS, a pulsed, focused, energetic ion beam bombards a surface, leading to interactions that cause the emission of positive and negative secondary ions.[33] The instrument used was a reflectron type time-of-flight mass spectrometer, with a design equivalent to that of the "ToF-SIMS IV".[34] An electron impact ion source (10 keV, $^{40}Ar^+$) was used for generating primary ion pulses for static ToF-SIMS. The pulsed ion beam was rastered over an area of 200 μm $\times$ 200 μm. The mass range was from 1 to 3500 amu, and the mass resolution $m/\Delta m$ was better than 4500 at mass 41. For charge compensation, a low-energy electron flood gun was utilized.

Streaming Potential Measurements. Streaming potentials[35,36] were measured in a rectangular microchannel cell consisting of two planar sample surfaces as published in a previous study.[37−40] The cell consisted of two Plexiglas parts and contained a sample holder, Pt electrodes, and channels for in- and outlet of the liquid. The samples were spin-coated PDMS on glass slides. The liquid flow between the sample surfaces in the cell was achieved by applying a pressure regulator and a transducer. All functions were monitored by a computer and a customized interface.

Results and Discussion

ToF-SIMS Results. As a first step, we should discuss the chemical composition of PDMS by ToF-SIMS to identify in detail the surface functional groups. Static secondary ion mass spectrometry (SSIMS)[41] has been used to characterize the structure of polymers on the basis of their fingerprint spectra that reveal specific spectroscopic features of the fragments located in the backbone and pendant groups. In the static ToF-SIMS regime, the emission of parentlike ion species (cationized: $[M + Me]^+$, protonated: $[M + H]^+$, deprotonated $[M - H]^-$, or loss of functional groups $[M - CH_3]^+$, $[M - OH]^+$, and so forth) or of molecular fragments is reached by very low total primary ion fluencies (10^{13} ions/cm^2).[42−44] Furthermore, molecule fragmentation can be reduced by using primary ion cluster beams such as Au_5^+ or Bi_3^+. In the present study, we used $^{40}Ar^+$ as the primary ion, which was adequate for the evaluation of the PDMS fragments.

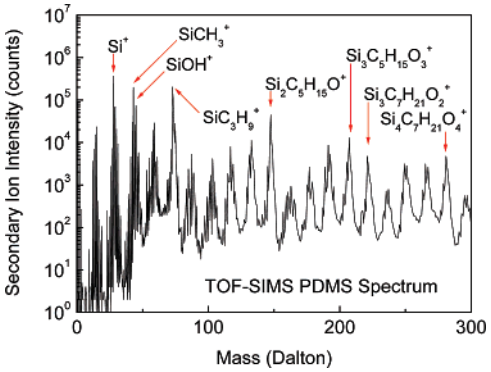

Figure 1. Representative ToF-SIMS spectrum of a UV/ozone-treated PDMS surface with characteristic secondary ion species.

ToF-SIMS has previously been used to study the molar mass distribution[45] and fragmentation mechanism of PDMS[46] in the high mass range. In the current analysis, various low-mass oxygen-containing fragments from the ToF-SIMS positive ion spectra were identified as representing the various possible oxygen effects seen in the chemical shift of the O 1s and Si 2p by XPS.[15] The ToF-SIMS spectra as obtained for various PDMS surfaces irradiated by UV/ozone were compared in detail. Differences in surface functionality across the whole sample series including the entire range of oxidation were identified by analysis of the low-mass range spectra. In Figure 1, extensive fragmentation can be observed in the mass range from 0 to 300 Da. The spectra recorded for varying exposure times of the PDMS surfaces are similar in this mass range. In the mass range below 100 Da, the dominant peak was at 73.05 Da, which corresponds to the mass of the major isotopes $(CH_3)_3Si^+$. Peaks at 43.00 Da (CH_3Si^+) and 27.98 Da (Si^+) can also be observed in the figure.

The relative intensities of the oxygen containing fragments from the positive ion spectra are collected in Table 1. The Si^+ peak intensity was chosen as an internal reference. Based on the data presented in Table 1, it could be concluded that, with increasing oxidation time, the silanol group was the major ionizable functional group favored, and the concentration of this surface entity was significantly enhanced when increasing the duration of the treatment time.

Adherence (Force Volume) Imaging by AFM. For FV imaging and subsequent AFM experiments, we employed Au-

(31) A force volume image contains an array of force curves over the entire sample area and is generated by ramping the z piezo as the tip scans across the area. Each force curve is measured at a unique $x-y$ position in the area, and force curves from an array of $x-y$ points are combined into a three-dimensional array, or "volume", of force data. The value at a point (x,y,z) in the volume is the deflection (force) of the cantilever at that position in space.

(32) Vancso, G. J.; Hillborg, H.; Schönherr, H. *Adv. Polym. Sci.* **2005**, *182*, 55.

(33) Benninghoven, A. *Angew. Chem., Int. Ed. Eng.* **1994**, *33*, 1023.

(34) Gunst, U.; Zabel, W. R.; Poll, G.; Arlinghaus, H. F. *Surf. Interface Anal.* **2004**, *36*, 1231.

(35) Delgado, A. V. *Interfacial Electrokinetics and Electrophoresis*; Marcel Dekker Ltd: New York, 2001.

(36) The streaming potential is defined as the difference in potential (V_{str}) at zero current caused by the flow of liquid under a pressure gradient in a capillary with flat walls made of the investigated specimen (PDMS).

(37) Van Wagenen, R. A.; Andrade, J. D. *J. Colloid Interface Sci.* **1980**, *76*, 305.

(38) Scales, P. J.; Grieser, F.; Healy, T. W. *Langmuir* **1990**, *6*, 582.

(39) Duval, J. F. L.; Huijs, G. K.; Threels, W. F.; Lyklema, J.; van Leeuwen, H. P. *J. Colloid Interface Sci.* **2003**, *260*, 95.

(40) Norde, W.; Rouwendal, E. *J. Colloid Interface Sci.* **1990**, *139*, 169.

(41) Arlinghaus, H. F. Static Secondary Ion Mass Spectrometry (SSIMS). In *Surface and Thin Film Analysis*; Bubert, H., Jenett, H., Eds.; Wiley-VCH: New York, 2002.

(42) Steffens, P.; Niehuis, E.; Friese, T.; Greifendorf, D.; Benninghoven, A. *J. Vac. Sci. Technol., A* **1985**, *3*, 1322.

(43) Benninghoven, A. *J. Vac. Sci. Technol., A* **1985**, *3*, 451.

(44) Bletsos, I. V.; Hercules, D. M.; Magill, J. H.; van Leyen, D.; Niehuis, E.; Benninghoven, A. *Anal. Chem.* **1988**, *60*, 938.

(45) Hagenhoff, B.; Benninghoven, A.; Barthel, H.; Zoller, W. *Anal. Chem.* **1991**, *63*, 2466.

(46) Dong, X.; Proctor, A.; Hercules, D. M. *Macromolecules* **1997**, *30*, 63.

Table 1. Relative Intensity ($\times 10^3$) of Positive Ions by ToF-SIMS for UV/Ozone-Treated PDMS Using Si^+ as a Standard

treatment time (min)	C^+	O^+	$SiCH^+$	$SiOH^+$	$SiCHO^+$	$SiC_2H_6O^+$	$SiC_2H_6O_2^+$
0	9.15	0.21	9.35	22.4	0.26	1.26	0.22
5	7.58	0.20	9.21	32.5	0.28	1.35	0.24
10	8.11	0.24	9.00	40.7	0.28	1.49	0.21
30	7.11	0.24	8.86	44.7	0.33	1.16	0.15
60	7.04	0.22	9.05	65.7	0.37	2.20	0.25

coated tips that were hydroxyl functionalized by thiol-based self-assembly and were reported to have stable and robust properties in CFM.[18,19] These tips met the two essential requirements for probing the particular pK_a features of the investigated surface: (a) they did not exhibit a pH-dependent change in ionization and (b) they were hydrophilic.[47] Figure 2 displays a typical FV image as obtained for a 30 min UV-treated PDMS surface in a phosphate buffer at two distinct pH values with a $\pm$20 nm resolution. Figure 2a shows a marked heterogeneous distribution of the surface functional entities introduced during the UV treatment. As revealed by the ToF-SIMS experiments and based on previous knowledge on the chemical nature (pK_a) of silanol functionalities,[48] it is suggested that the adherence variation observed by CFM at low pH values was related to a heterogeneous distribution of protonated silanol functional groups ($-SiOH_2^+$). We have added representative pull-off force curves showing pull-off events in bright-colored, low-adherence domains (Figure 2c, curve (1)) and in dark-colored, high-adherence domains (Figure 2c, curve (2)). The typical size of the high adherence domains lies in the range 20$-$100 nm. When the pH of the buffer system was adjusted to 7.2, the adherence displayed a dramatic decrease and clearly revealed a homogeneous distribution of adherence over the entire sample surface (Figure 2b). Typical corresponding force curves are shown in Figure 2d. A gradual increase of the solution pH caused deprotonation of the silanol groups, and the surface then became more negatively charged. This caused electrostatic (dipolar) repulsion between the tip and the ionized surface, as reflected in Figure 2b and d. To further investigate the surface ionization state, FV imaging was performed on various UV/ozone-irradiated PDMS samples immersed in electrolytes as a function of the solution pH.

Force Titration. For oxidized PDMS films, Hillborg et al.[21] showed that the mean roughness (R_a) was not influenced by the UV/ozone exposure, so that only a minor influence of the sample topography on the force measurements was expected.[49] To analyze the pull-off force distributions over the imaged sections, data were plotted in the form of force histograms at various pH values (compare Figure S1, shown in the Supporting Information). The most probable values of the pull-off forces, which correspond to the peak in the Gaussian statistics, were plotted as a function of pH to yield force titration curves as those shown in Figure 3. The force titration curves for the exposed samples exhibited a typical sigmoidal pattern. The force values decreased with increasing exposure time, from 13 nN (untreated) to 4 nN (treated for 1 h) at low pH and from 12 nN (untreated) to 0 nN (treated for 1 h) at high pH. However, untreated PDMS exhibited a high and almost constant pull-off force of 12$-$13 nN over the entire pH range investigated.

The trends in the average pull-off force for low pH values as a function of treatment time should be discussed at this juncture. To this end, we first need to recall the variation of the surface elastic modulus for PDMS during treatment. UV/ozone-treated PDMS samples have been shown to exhibit increasing surface elastic moduli with increasing treatment doses.[21] Such an increasing modulus influences the contact area and indentation depth between the CFM tip and the sample. The elastic deformation of PDMS in the absence of external normal forces is determined by the adhesive interactions between the tip and the surface.[50,51]

Figure 4 shows the force versus indentation plots for a Si_3N_4 AFM tip interacting with (a) an untreated PDMS surface and (b) PDMS exposed to 60 min of UV/ozone. From the approaching part of the force versus indentation curve, it can be easily inferred that untreated PDMS had a larger adhesion-induced indentation than the oxidized sample. At the same maximum load, the oxidized PDMS surface showed less indentation. For a pyramidally shaped AFM tip, this smaller indentation results in a decrease in the effective contact area. Moreover, from the retracting part of the force versus indentation curves, it could be seen that untreated PDMS, as compared to the treated sample, was deformed and "pulled up" by the tip over a longer distance before the AFM tip detached.

Compared to a UV/ozone-treated sample, pure PDMS has free polymer chains with high segmental mobility in the probed surface region, which effectively increases the friction force as a result of an adhesive interaction between the tip and the viscoelastic surface during the pull-off event. This friction force corresponds to a significant contribution in the force balance. The increased friction force and the increased effective contact area between the tip and the surface can account for the higher pull-off forces for the untreated samples and the samples with lower treatment times.

For UV/ozone-treated samples, the interactions between the ionizable functional (silanol) groups and the hydroxyl groups at the tip influence the magnitude and the pH dependence of the pull-off force. Since the hydroxyl-terminated functionalized tips did not show any pH dependence, the titration behavior could be directly attributed to varying degrees of protonation of the silanol groups at the PDMS surface. Based on the force titration curves, it was apparent that the strength of adhesion and the extent of attractive interaction diminished with increasing pH. To reduce the influence of variations concerning the tip radius and contact area, the normalized pull-off force values were calculated by dividing the actual values with the pull-off force value obtained for the original nontreated PDMS pull-off force.

Normalized pull-off force data for the Si_3N_4 tips and for the hydroxyl-functionalized tips at pH = 3 are compared in Figure 5. After 5 min of UV/ozone treatment, the average pull-off force decreased to 55% of the initial value when using Si_3N_4 tips and to 15% of the initial value when using hydroxyl-terminated tips. This large difference is a strong indication of hydrogen bond formation between the surface of the oxidized PDMS and the hydroxyl-terminated tips. Such hydrogen bonding was nearly absent in the case of the Si_3N_4 tips.

The transition pH range from complete protonation (low pH values) to complete deprotonation (high pH values) of the silanol groups (compare Figure 3) was clearly reflected in the force titration curves. The corresponding inflection points, denoted as p$K_{1/2}$ at which value half of the surface sites were ionized (as obtained from force curves versus pH), were used to estimate the surface effective thermodynamic equilibrium constant. Its value at the inflection point for PDMS studied, denoted hereinafter as pK_a, was evaluated from the force titration curves and lies in

(47) Vezenov, D. V.; Noy, A.; Rozsnyai, L. F.; Lieber, C. M. *J. Am. Chem. Soc.* **1997**, *119*, 2006.
(48) Parks, G. A. *Chem. Rev.* **1965**, *65*, 177.
(49) Eaton, P. J.; Graham, P.; Smith, J. R.; Smart, J. D.; Nevell, T. G.; Tsibouklis, J. *Langmuir* **2000**, *16*, 7887.
(50) Sun, Y. J.; Walker, G. C. *Langmuir* **2005**, *21*, 8694.
(51) Sun, Y. J.; Akhremitchev, B.; Walker, G. C. *Langmuir* **2004**, *20*, 5837.

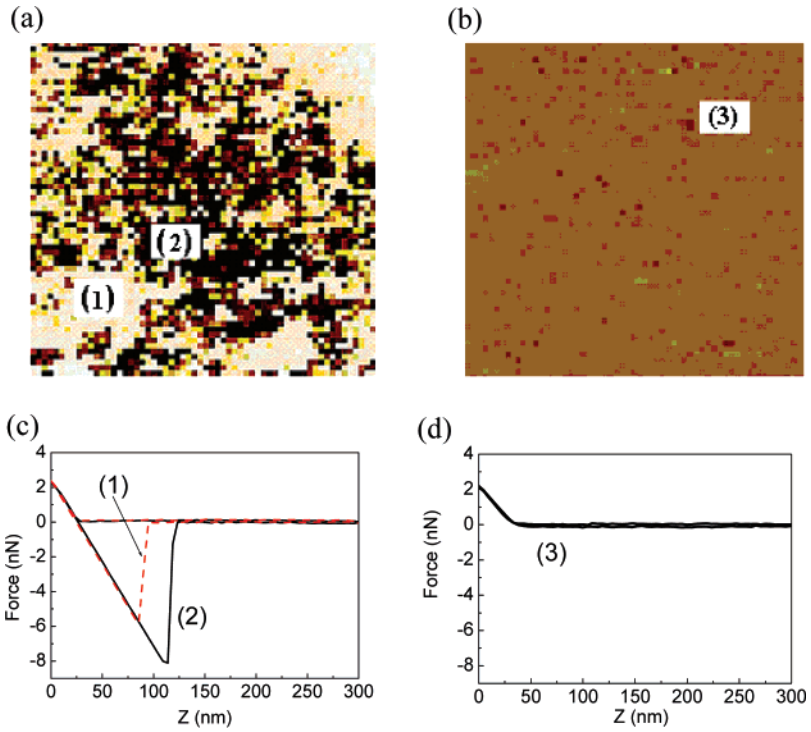

Figure 2. Contact mode AFM force volume images of a PDMS surface after 30 min of UV/ozone treatment in phosphate buffer solution (ionic strength = 300 mM) at (a) pH = 3, $F_{\text{pull-off}} = 8.06 \pm 0.97$ nN and (b) pH = 7.2, $F_{\text{pull-off}} = 0.20 \pm 0.10$ nN. The color scale ranges from dark (high adherence) to bright (low adherence). Scan size: 500 nm × 500 nm. The *Z* range of the force volume was 20 nm. (c) Typical force curve from a region with (1) low and (2) high adherence at pH = 3. (d) Typical force curve obtained for the same surface at pH = 7.2.

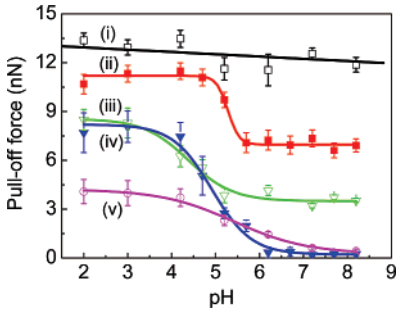

Figure 3. Chemical force titration curves showing the adhesive force between the hydroxyl-functionalized tips and the treated PDMS samples as a function of solution pH. Error bars represent the standard deviation in the adherence as obtained from the force volume images. The solid lines have been added as guides to the eye. (i) Untreated PDMS (□); (ii) PDMS treated for 5 min (■); (iii) PDMS treated for 15 min (▽); (iv) PDMS treated for 30 min (▼); (v) PDMS treated for 60 min (○).

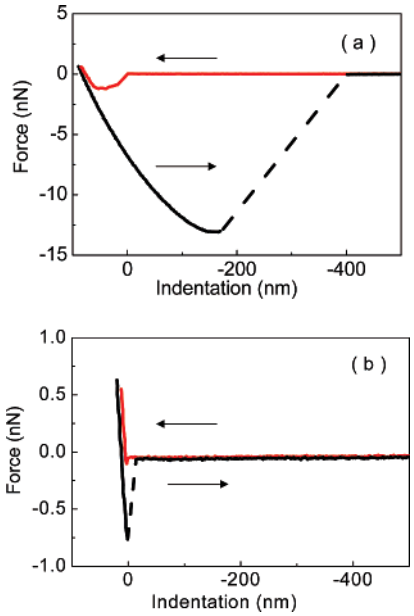

Figure 4. Typical plots representing AFM force versus indentation for a Si_3N_4 tip interacting with (a) an untreated PDMS surface and (b) a PDMS surface treated for 60 min. Both sets of data were obtained at pH = 3.

the range 4.5−5.5, depending on the treatment dose. Based on the surface site dissociation theory and the Gouy−Chapman−Stern double layer models, as proposed by Yates,[29,52] and later extended by Davis[53,54] and James,[55] the relevant protolytic reactions of −SiOH groups may be summarized as follows:

$$-\text{SiOH}_2^{+} \leftrightarrow -\text{SiOH} + \text{H}_s^{+} \qquad K_{a_1} \qquad (1)$$

$$-\text{SiOH} \leftrightarrow -\text{SiO}^{-} + \text{H}_s^{+} \qquad K_{a_2} \qquad (2)$$

where K_{a_1} and K_{a_2} are the constants associated to the protolytic reactions 1 and 2, respectively. From the literature,[56,57] pK_{a_1} is

(52) Yates, D. E.; Healy, T. W. *J. Colloid Interface Sci.* **1976**, *55*, 9.
(53) Davis, J. A.; James, R. O.; Leckie, J. O. *J. Colloid Interface Sci.* **1978**, *63*, 480.
(54) Davis, J. A.; Leckie, J. O. *J. Colloid Interface Sci.* **1978**, *67*, 90.
(55) James, R. O.; Davis, J. A.; Leckie, J. O. *J. Colloid Interface Sci.* **1978**, *65*, 331.

(56) (a) Ong, S. W.; Zhao, X. L.; Eisenthal, K. B. *Chem. Phys. Lett.* **1992**, *191*, 327. (b) Lyklema, J. *Fundamentals of Interface and Colloid Science*; Academic Press: San Diego, CA, 1995; Vol. II.
(57) Wang, B.; Abdulali-Kanji, Z.; Dodwell, E.; Horton, J. H.; Oleschuk, R. D. *Electrophoresis* **2003**, *24*, 1442.

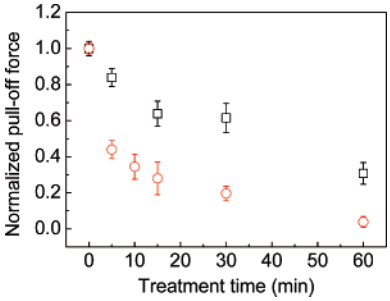

Figure 5. Normalized pull-off force between the AFM tip and the PDMS surface as a function of UV/ozone treatment time (t). The force values were normalized with respect to the force obtained for the untreated specimen ($t = 0$) at pH = 3. Interactions with a hydroxyl-functionalized tip (□); interactions with a Si_3N_4 tip (○).

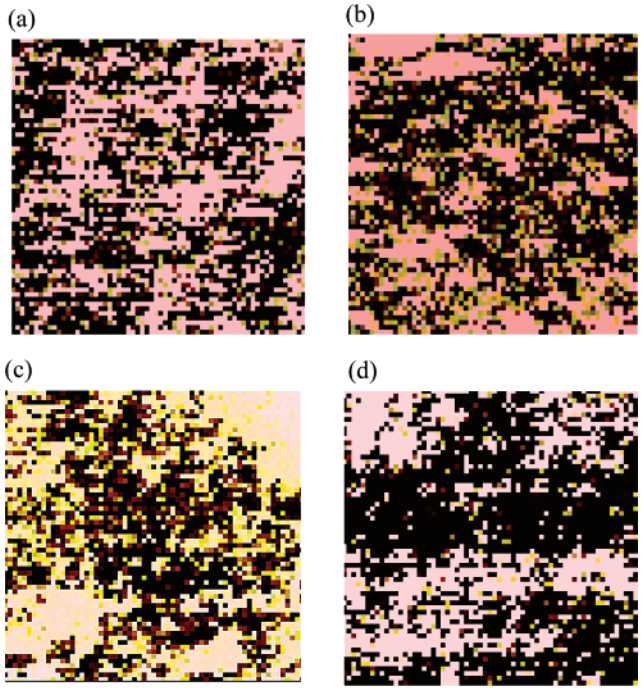

Figure 6. Contact mode AFM force volume images of oxidized PDMS surfaces in a phosphate electrolyte solution (pH = 3) obtained with a hydroxyl-terminated tip. Scan size: 500 nm × 500 nm. The color scale ranges from dark (high pull-off, high adherence) to bright (low pull-off, low adherence). The Z range of the force volume was 20 nm. (a) 5 min UV/ozone treatment ($F_{pull-off} = 11.33 \pm 0.52$ nN); (b) 15 min UV/ozone treatment ($F_{pull-off} = 8.29 \pm 0.92$ nN); (c) 30 min UV/ozone treatment ($F_{pull-off} = 8.06 \pm 0.97$ nN); (d) 1 h UV/ozone treatment ($F_{pull-off} = 3.99 \pm 0.77$ nN).

~1 and pK_{a_2} is ~4. In our force titration experiments, the surface effective pK_a was obviously shifted to higher pH values and no significant or systematic variation with treatment time could be unambiguously established.

Surface pK_a Shift. In Figure 6, the representative force volume images of UV/ozone-treated PDMS are shown as a function of treatment time. The characteristic size of the hydrophilic domains (dark areas in the images) was within the range of 20−200 nm. The ionizable silanol groups were surrounded in their molecular environment by hydrophobic methyl groups. Similar to previous studies,[25,58] we propose that, for the UV/ozone-treated PDMS surfaces, the silanol groups were stabilized by the surrounding methyl groups, leading to the deprotonation occurring at higher pH values, as compared to those for the listed homogeneous silanol surface.[56,57]

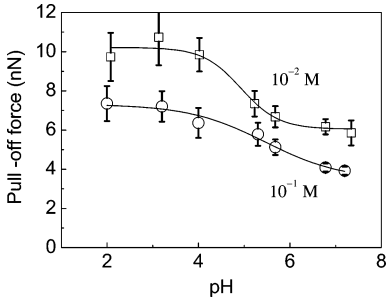

Figure 7. Force titration curves for a PDMS surface oxidized for 15 min in a phosphate buffer at two ionic strengths.

Moreover, we also consider the possibility of intermolecular lateral hydrogen bond formation between the surface silanol groups. In Figure 6, it can be clearly seen that the −SiOH-rich hydrophilic domains were, on average, larger for the samples exposed to UV/ozone for 1 h, as compared to those exposed for 5 min. The aforementioned intermolecular lateral hydrogen bonding may cause the acidic protons to be held more tightly on the surface, resulting in the dissociation of the functional group at higher pH values. Furthermore, in Figure 3, the pK_a transition range for the sample exposed to UV/ozone for 1 h appears to be broader than that for the sample exposed for merely 5 min. This is in line with the aforementioned explanation.

In addition to the previously mentioned stabilization effects, another possible explanation could be the influence of a double layer at the polymer surface giving rise to a shift in the pK_a to higher pH values. Figure 7 shows the force titration curves measured at two different ionic strengths (10^{-2} M and 10^{-1} M) using phosphate buffer solutions. For the higher ionic strength solution, the magnitude of the pull-off force was reduced. It is likely that, for the corresponding high electrolyte concentrations, the counterions screened the surface functional groups taking part in the interactions with the −OH tip, resulting in lower pull-off forces. Moreover, the transitions from low to high pH ionization states broadened with increasing ionic strength. As can also be seen in Figure 7, no clear shift for the surface pK_a was observed when varying the electrolyte concentration. Despite the uncertainty inherent to the experimental data, the latter result suggests that, for the system under study, the impact of the double layer (surface proton concentration as compared to bulk proton concentration) on the stabilization of the surface charge was not predominant.

Streaming Potential Experiment in NaCl Solutions. To gain further understanding of the surface ionization behavior of oxidized PDMS surfaces, streaming potential measurements were carried out on PDMS with varying degrees of oxidation (i.e., treated with UV/ozone for various exposure times) at different pH values in 10^{-2}, 10^{-3}, or 10^{-4} M aqueous sodium chloride and phosphate solutions. From the linear dependence of the measured streaming potential with the applied pressure drop, one can determine the electrokinetic potential, also called the zeta potential (ζ) for the surface under investigation.[59] It should be noted that the PDMS surface was assimilated to a rigid, ion-impenetrable surface with *a priori* a well-defined location for the slip plane and thus a clear physical meaning for the electrokinetic potential.[60] This rigid nature of PDMS was justified by the very low water

(58) Schönherr et al. (see ref 25) previously suggested that the surface pK_a of −COOH groups introduced on oxyfluorinated isotactic polypropylene shifted to higher values as compared to the bulk pK_a. The observed shifts in pK_a were due to the presence of a surrounding hydrophobic environment, which retarded the ionization process.

(59) Werner, C.; Kärber, H.; Zimmermann, R.; Dukhin, S.; Jacobasch, H. J. *J. Colloid Interface Sci.* **1998**, *208*, 329.

(60) Duval, J. F. L.; Ohshima, H. *Langmuir* **2006**, *22*, 3533.

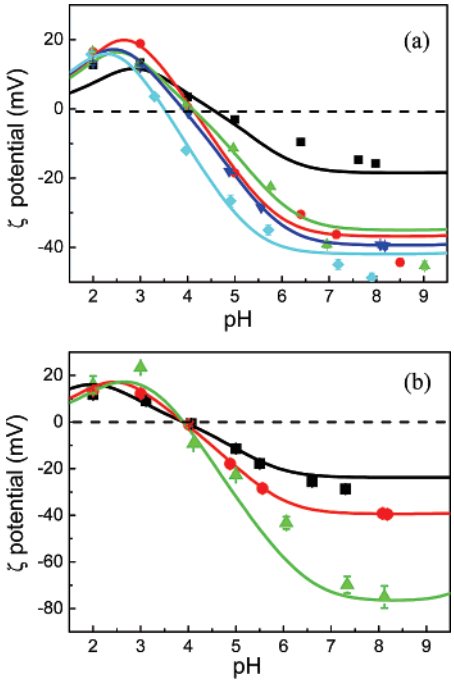

Figure 8. (a) ζ potential versus pH for varying treatment times of PDMS with a 10^{-3} M NaCl electrolyte solution. The points represent experimental data, and the solid lines correspond to simulation results according to the double layer model outlined in the Supporting Information. Untreated PDMS (■); PDMS treated for 5 min (●); PDMS treated for 15 min (▲); PDMS treated for 30 min (▼); PDMS treated for 60 min (◆). (b) ζ potential versus buffer pH for a 30 min oxidized PDMS surface as measured in a NaCl solution at various ionic strengths. The points represent the experimental data, and the solid lines correspond to simulation results according to the double layer model outlined in the Supporting Information. NaCl: 10^{-2} M (■); 10^{-3} M (●); 10^{-4} M (▲).

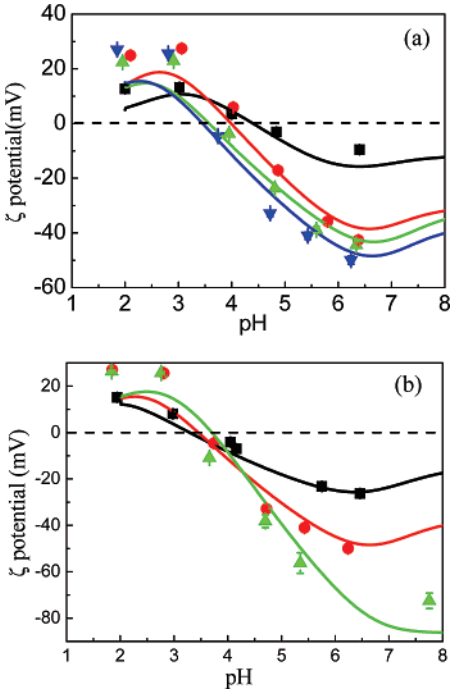

Figure 9. (a) ζ potential versus buffer pH for various treatment times of PDMS with a 10^{-3} M phosphate salt electrolyte solution. The points represent experimental data, and the solid lines correspond to simulation results according to the double layer model outlined in the Supporting Information. Untreated PDMS (■); PDMS treated for 5 min (●); PDMS treated for 15 min (▲); PDMS treated for 30 min (▼). (b) ζ potential for a 15 min oxidized PDMS sample measured with phosphate solution at various ionic strengths. The points represent experimental data, and the solid lines correspond to simulation results according to the double layer model outlined in the Supporting Information. Phosphate salt buffer: 10^{-2} M (■); 10^{-3} M (●); 10^{-4} M (▲).

permeability, as reported in the literature,[61] for PDMS substrates used in microfluidic devices to prevent leakage.[62,63] Also, the positioning of the relevant ionogenic silanol groups, responsible for the PDMS surface charge, within a 1−2 nm top layer,[18] was in line with the notion of surface charge density as classically used for impermeable materials (for soft objects, the electrokinetic features are interpreted in terms of space charge density). All these elements basically justify the use of the classical Smoluchowski equation which becomes approximate when dealing with substrates such as gels or charged polyelectrolytes for which flow penetration (or hydrodynamic permeability) is significant.[64]

In Figure 8a, ζ potential values as a function of pH are shown for samples in a 10^{-3} M NaCl electrolyte solution. The lines in Figure 8a correspond to simulation results obtained using the double layer model outlined in the Supporting Information. The ζ potential values were positive at low pH since the surface was positively charged, and they were found to decrease with increasing pH due to the gradual deprotonation of the surface silanol groups. After passing the isoelectric point (IEP), where $\zeta = 0$, a negative potential was reached (negatively charged surface). The IEP was estimated from the sigmoidal shape of the curves. Moreover, around the IEP, the slopes of these curves increased with increasing treatment time. This behavior indicates an increasing number of surface-ionizable groups with treatment time, as previously shown by the ToF-SIMS experiments mentioned earlier.

All the observed IEP values were higher than the values reported in the literature for silanol groups on silica surfaces (IEP ≈ 2−2.5).[56] The shift of the IEP with treatment time may be related to the heterogeneity of the surface (hydrophobic/hydrophilic balance) and/or to specific ion adsorption (Na^+ or Cl^-) onto the PDMS surface. To discriminate between these two processes, streaming potential experiments were performed at various levels of NaCl concentrations. Figure 8b shows the pH dependence of the ζ potential as a function of pH for three ionic strengths obtained from NaCl buffer solutions for samples oxidized for 30 min. At a given pH, the magnitude of the ζ potential decreased with increasing ionic strength. This is consistent with expectations from the classical double layer theory (i.e., increased amounts of ions in the solution increase the surface charge screening).[65] Furthermore, the IEP did not show any measurable variations when varying the salt level in the solution. This excludes the impact of the NaCl ionic specificity for PDMS on the IEP variations with UV/ozone time exposure.

Streaming Potential Experiments in Phosphate Buffer Solutions. To mimic the conditions of the AFM experiments, a phosphate salt buffer was also used as the electrolyte solution in the streaming potential measurements. Figure 9a shows the resulting ζ potentials for varying treatment times of PDMS with a 10^{-3} M ionic strength phosphate salt at different pH values. The overall shape of the ζ−pH curves was similar to those obtained with the NaCl electrolytic solution. The associated IEP

(61) Graubner, V. M.; Jordan, R.; Nuyken, O.; Kötz, R.; Lippert, T.; Schnyder, B.;Wokaun, A. *Polym. Mater. Sci. Eng.* **2003**, *88*, 489.
(62) Sia, S. K.; Whitesides, G. M. *Electrophoresis* **2003**, *24*, 3563.
(63) McDonald, J. C.; Whitesides, G. M. *Acc. Chem. Res.* **2002**, *35*, 491.
(64) Duval, J. F. L.; Wilkinson, K. J.; van Leeuwen, H. P. *Environ. Sci. Technol.* **2005**, *39*, 6435.
(65) Tadros, T. F.; Lyklema, J. *J. Electroanal. Chem.* **1968**, *17*, 267.

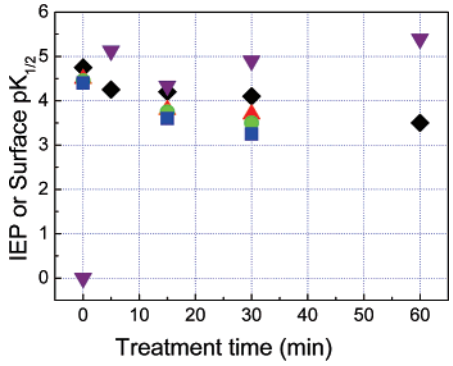

Figure 10. Summary of the IEP (ref 60) and surface pK_a values as obtained for UV/ozone-treated PDMS surfaces. The IEP was evaluated from streaming potential experiments. Buffers: NaCl (◆); 10^{-2} M (■), 10^{-3} M (●), and 10^{-4} M (▲) phosphate salt. Surface pK_a as obtained by an AFM titration curve in a 0.3 M phosphate buffer solution (▼).

values also decreased as a function of the treatment time but quantitatively differed from those determined for PDMS in the presence of NaCl. Furthermore, Figure 9b shows the ζ potential for a PDMS sample oxidized for 15 min as measured with a phosphate solution at various ionic strengths. As opposed to that for the NaCl electrolyte solution, the IEP decreased upon increase of the ionic strength of the phosphate solution. This indicates an occurrence of anion adsorption onto the PDMS surface.

Comparison of the Streaming Potential and AFM Results. Streaming potential and AFM force titration experiments were used to characterize the surface ionization state of untreated and UV/ozone-irradiated PDMS on varying length scales. Streaming potential data are averaged over large sample areas (on the order of cm^2), and the surface IEP is used as a characteristic ionization state parameter. This is compared to the surface pK_a determined on the nanoscale by AFM force titration experiments. In the case of AFM, the probed area had a characteristic size of 20−30 nm. It was found from the streaming potential experiments that there were low amounts of charge at the pure PDMS surface. This can be explained by pointing out that the PDMS precursor, Sylgard 184 (Dow Corning), contains a reinforcing silica filler, and the hydrolysis of this silica in an aqueous electrolyte environment would introduce some surface charge. In contrast, in the AFM titration curves, we could not find any pH dependent behavior for the untreated samples. As mentioned before, the pull-off force obtained included both hydrogen bond interactions as well as van der Waals forces between the tip and the sample. For untreated PDMS samples, the pull-off forces were predominantly determined by the van der Waals interactions and did not show titration behavior with variations in pH.

A summary of the IEP and surface pK_a values for the UV/ozone-treated PDMS surfaces is visualized in Figure 10. It can be seen that the IEP values in NaCl solution decreased with increasing treatment time, approaching the reported literature data. This indicates that the surface heterogeneity was reduced with treatment time, proceeding toward a more homogeneous silanol-functionalized surface. In addition, there were clear differences between the two buffers (NaCl and phosphate) and those differences were strongly dependent on the UV/ozone exposure time. Overall, the IEP values in the phosphate solution were lower than those in the NaCl solution. This IEP shift in the phosphate buffer suggested that *specific anions* were adsorbed onto the surface and that the phosphate anions therefore could contribute to the double layer charging taking place at the PDMS surface. Furthermore, whereas the IEP of NaCl buffered systems did not show any dependence on ionic strength, the phosphate

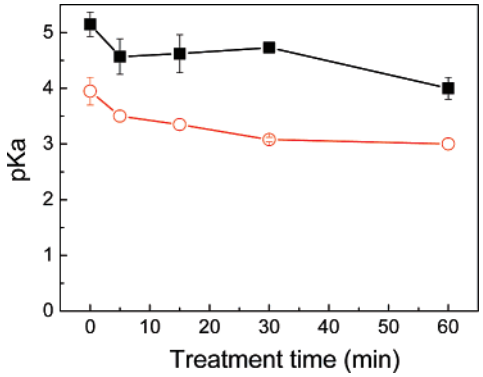

Figure 11. Values of pK_{a_1} (○) and pK_{a_2} (■) as obtained by the double layer model outlined in the Supporting Information. Electrolyte: NaCl.

buffered system did. In other words, the IEP decreased to a certain extent when the phosphate concentration increased and this was as a result of (mono- and multivalent) anionic ($H_2PO_4^-$ and HPO_4^{2-}) surface adsorption (see the Supporting Information). Thus, on average, more than one electron charge was added to the surface per adsorbed ion. With increasing ionic strength of the buffer, the magnitude of the specific adsorption increased, making the surface more negatively charged. This explains the difference between the electrokinetic results as obtained for the NaCl buffer versus for the phosphate buffer.

In Figure 10, one can see that both the IEP and the "effective surface pK_a" values in phosphate buffer changed with increasing treatment dose and were higher than the values published in the literature for silanol (see related discussion above). However, the differences between the IEP and the effective surface pK_a should be noticed and explained as follows. The IEP value was obtained in a "direct" manner from the analysis of the surface charge, while the effective force pK_a was derived on the basis of analyzing differences in the pull-off force. Thus, the measurement and interpretation of the adherence remain difficult in view of the uncertainties pertaining to the tip shape and surface roughness (use of granular gold coating).[66] The surface parameters were averaged according to radically different ways since the physical−chemical processes probed by either electrokinetics or AFM were on different scales, that is, macro versus nano, respectively.

Referring to the surface charge formation mechanism expressed in eqs 2 and 3, the relationship between the IEP and the surface ionization pK_a values can be expressed as

$$\mathrm{IEP} = {}^1/_2(\mathrm{p}K_{a_1} + \mathrm{p}K_{a_2}) \qquad (3)$$

Relation 3 is valid for indifferent electrolyte solutions. By applying the Gouy−Stern equation with the site dissociation model, as described in the Supporting Information, the values for pK_{a_1} and pK_{a_2} could be obtained by fitting the streaming potential data obtained in an indifferent NaCl electrolyte with least-square regression (LSR) methods. The values obtained are shown in Figure 11. It was found that both pK_{a_1} and pK_{a_2} were higher than the values suggested in the literature, as previously mentioned. With an increase in the treatment dose, pK_{a_1} and pK_{a_2} were shifted to more acidic values. These values were subsequently considered for the quantitative analysis of the electrokinetic data measured in phosphate buffer solutions (see below).

Taking into account specific ion adsorption, a modified site dissociation model was applied (shown in the Supporting

(66) Hu, K.; Bard, A. J. *Langmuir* **1997**, *13*, 5114.

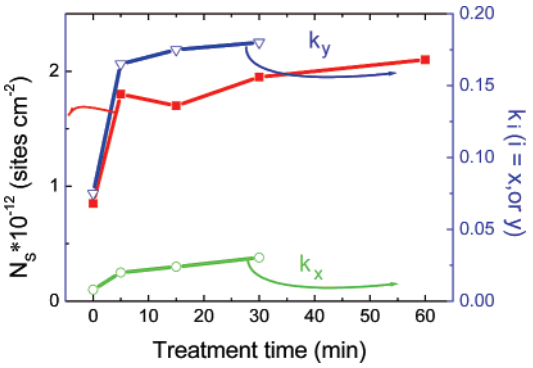

Figure 12. Number of active surface sites, denoted N_S, in a buffer solution (■) and the specific ion adsorption parameters k_x (○) and k_y (▽) defined by $k_x = RT \ln(K_x)/F$ and $k_y = RT \ln(K_y)/2F$ (with R, T, and F in SI units) as a function of treatment time for UV/ozone-treated PDMS. Electrolyte: 10^{-3} M phosphate buffer.

Information). In this model, we further include two types of specifically adsorbed ions onto the treated sample surface.

$$-SiOH_2^+ + H_2PO_4^- \overset{K_x}{\Leftrightarrow} -SiOH_4PO_4 \quad (4)$$

$$-SiOH + HPO_4^{2-} \overset{K_y}{\Leftrightarrow} -SiOH_2PO_4^{2-} \quad (5)$$

Here, K_x and K_y are the corresponding equilibrium constants. Figure 12 shows the simulation results based on this ion-exchange equilibrium mechanism. The parameter N_s denotes the total number of active surface sites. It was found that N_s increased with an increasing dose of the UV/ozone treatment. In addition, the values of the specific ion adsorption equilibrium constants K_x and K_y also increased. These results confirm that, for higher concentrations of the ionizable sites, specific ion adsorption took place to a larger extent. Similarly, on a molecular scale, it seems possible that the phosphate ion adsorption contributes to the local double layer composition although it was very difficult to picture this in a quantitative way on the basis of merely the AFM titration curves. Returning to Figure 7, the broadening of the transition area with increasing strength of the ionic solution may be due to the specific phosphate ion adsorption at the surface, which altered the adherence between the tip and the functional groups.

Conclusions

The average chemical composition of UV/ozone-treated PDMS was monitored by ToF-SIMS in a quantitative way. Corresponding results showed that silanol functional groups were the most probable ionizable groups on the surface. Their concentration increased with increasing treatment time. AFM pull-off force measurements were carried out on oxidized PDMS films as a function of pH by using hydroxyl-functionalized tips. A change in the surface charge induced by the dissociation of silanol groups could be detected by monitoring the adhesive forces between the surface and the modified AFM probes. Laterally resolved force "imaging" gave clear evidence for heterogeneous functional group distributions over the surface of the oxidized samples. Oxidized hydrophilic patches (initially 20−100 nm in size) grew with increasing treatment time. Force titration curves revealed that the effective surface pK_a values were in the range 4.5−5.5. This was higher than the typical literature value of uniform silanol groups on a silica surface. We concluded that this shift was primarily due to the hydrophobic environment having stabilizing effects on the surface ionization. The broadening of the pK_a range that could be observed with increasing treatment dose was interpreted as a result of an increasing probability of intermolecular hydrogen bonding and specific ion adsorption. By interpreting streaming potential experiments on the basis of a Gouy−Stern site dissociation model, it was confirmed that specific ion adsorption took place in phosphate electrolyte solutions, thus contributing to the overall (as probed by electrokinetics) and local (as probed by AFM) states of ionization of the surface silanol groups.

Acknowledgment. The authors gratefully acknowledge financial support from the Dutch Polymer Institute. Dr. Holger Schönherr is acknowledged for helpful discussions and comments. Finally, Dr. Nikodem Tomczak is acknowledged for designing a custom-built Labview application for AFM force volume image analysis.

Supporting Information Available: Representative histograms of the pull-off force recorded for PDMS exposed to 30 min UV/ozone at different pHs and details of the quantitative study of specific ion adsorption on an oxidized PDMS surface using the Gouy−Stern double layer with site dissociation model. This material is available free of charge via the Internet at http://pubs.acs.org.

LA063168S

Surface Ionization State and Nanoscale Chemical Composition of UV-Irradiated Poly(dimethylsiloxane) Probed by Chemical Force Microscopy, Force Titration and Electrokinetic Measurements

*Jing Song[1], Jérôme F.L. Duval[2], Martien A. Cohen Stuart[3], Henrik Hillborg[1, 4], Ullrich Gunst[5], Heinrich F. Arlinghaus[5], G. Julius Vancso[1]**

[1]University of Twente, Dutch Polymer Institute and MESA$^+$ Institute for Nanotechnology, Materials Science and Technology of Polymers, P.O. Box 217, 7500 AE Enschede, The Netherlands

[2]*Laboratory Environment and Mineral Processing, Nancy-University, CNRS, Research Center Francois Fiessinger, 15 Avenue du Charmois, BP40, 54501 Vandoeuvre-lès-Nancy cedex, France*

[3]*Laboratory of Physical Chemistry and Colloid Science, Wageningen University P.O. Box 8038, 6700 EK Wageningen, The Netherlands*

[4]*ABB AB, Corporate Research, Power Technology, Västerås, SE 72178, Sweden*

[5]*Physikalisches Institut, Wilhelm-Klemm-Str. 10, Westfälische Wilhelms-Universität D-48149 Münster, Germany*

Email: j.song@tnw.utwente.nl, g.j.vancso@tnw.utwente.nl

Supporting information

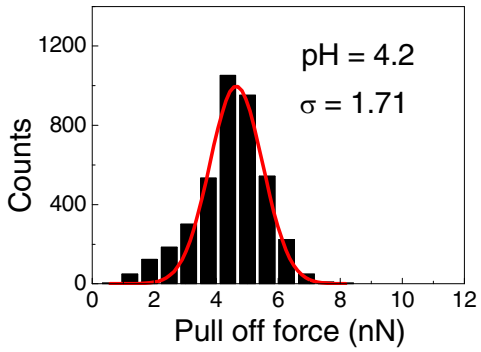

Error! Bookmark not defined.

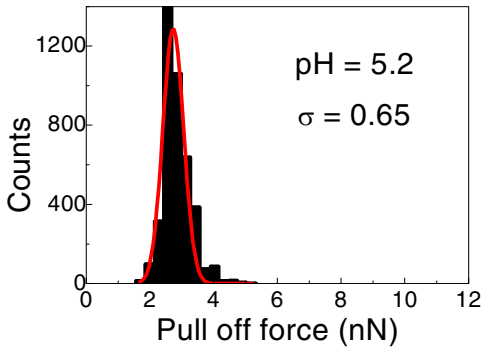

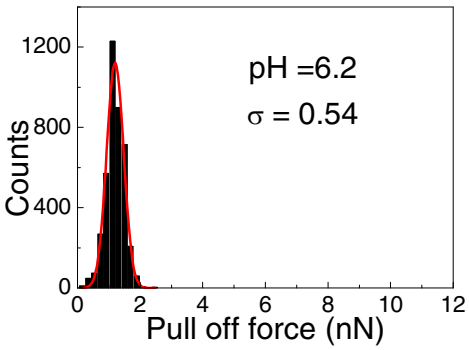

Figure S1. Representative histograms of the pull-off force recorded for PDMS exposed to 30 min UV/Ozone at different pH. Scan size: 500 nm × 500 nm (4096 force curves per histogram). The histograms were fitted using a Gaussian distribution (σ = standard deviation).

As shown in Figure S1, it is clear that when using a hydroxyl functionalized tip, the average pull-off force decreases with increasing pH. The histograms are fitted according to a Gaussian statistical distribution. The standard deviation of the Gaussian distribution (σ) decreases from 1.93 to 0.54 with increasing pH reflecting a more homogenous distribution of pull off force.

Gouy–Stern Double Layer with Site Dissociation Model

Classical Gouy–Stern Double Layer

Anisotropic ion accumulation exists at the contact interface between an electrochemically active surface and a liquid electrolyte.[1] The charges at and adjacent to the surface will cause a potential difference between the region near the surface and the bulk of the solution. The potential decreases within the solution as a function of the distance from the charged surface. Specific ion adsorption occurrence is inferred from the dependence of certain double layer properties on the natures of counter and co-ions. Generally, ions that interact specifically (non-electro statically) with the surface approach it at a shorter distance.

The charge balance as a whole is written as

$$\sigma^0 + \sigma^d + \sigma^{ads} = 0 \tag{s1}$$

σ^0 is the surface charge; σ^d is the diffuse charge; σ^{ads} is the charge that stems from the adsorbed ions.

If $\sigma^{ads} = 0$, there is no specific ion adsorption.

The stern layer acts as a molecular condenser represented by a capacitance *C*. The surface potentials ψ^0, the potential at the oHp ψ^d and the surface charges σ^d are related via the capacitances.[1]

$$C = \frac{\mathrm{d}\sigma^d}{\mathrm{d}(\psi^0 - \psi^d)} \tag{s2}$$

The plane where these specifically adsorbed ions reside is called the inner Helmholtz plane (iHp). The iHp layer capacitance and the oHp layer capacitances are given by

$$C_1 = \frac{\mathrm{d}\sigma^0}{\mathrm{d}(\psi^0 - \psi^\beta)} \tag{s3}$$

and

$$C_2 = \frac{\mathrm{d}\sigma^d}{\mathrm{d}(\psi^\beta - \psi^d)} \tag{s4}$$

respectively.

ψ^β is the potential at the inner Helmholtz plane. Within the framework of our analysis, the capacitance is considered constant (integral capacitances are then assimilated to differential capacitances), as commonly adopted in the literature.[1]

Case Modeling: No Specific Ion-Adsorption

For the description of charge and potential at the oxide-electrolyte interface, different models can be used.[1-3] The surface charge at the oxidized PDMS-electrolyte interface originates from the dissociation of silanol groups when in contact with a NaCl buffer solution. The equilibrium constants of silanol ionization processes are K_{a1} and K_{a2} given by

$$K_{a1} = \frac{[-SiOH][H^+]\exp(-e\psi^0/kT)}{[-SiOH_2^+]} \tag{s5}$$

$$K_{a2} = \frac{[-SiO^-][H^+]\exp(-e\psi^0/kT)}{[-SiOH]} \tag{s6}$$

where $\left[H^+\right]$ is the concentration of protons in the bulk and the other quantities in brackets are surface concentrations; *k* is the Boltzmann factor; *T* is the absolute temperature, ψ^0 is the surface potential and *e* is the elementary charge.

Surface charge σ_0 derives from the acid-base interactions of the solution components and is defined by

$$\sigma_0 = e\left(\left[-SiOH_2^+\right]-\left[-SiO^-\right]\right) \tag{s7}$$

Consequently the pH of the solution is the primary externally adjustable variable, which together with the electrolyte concentration determines the sign and the magnitude of σ_0. In this study, neither formation nor disappearance of silanol groups is taken into account and the parameter *Ns* (effective number of ionizable surface sites) is therefore supposed to remain constant upon changing the electrolyte composition. The total amount of reactive silanol groups is directly dependent on the UV/Ozone treatment dose. We have

$$Ns = \left[-SiOH_2^+\right]+\left[-SiO^-\right]+\left[SiOH\right] \tag{s8}$$

Diffuse ionic charge σ^d can be derived from the Gouy–Chapman theory for a 1:1 electrolyte.

$$\sigma^d = -\left(8I\varepsilon_0\varepsilon_{rw}RT\right)^{1/2}\sinh\left(y^d/2\right) \tag{s9}$$

where ε_0 is the dielectric permittivity of vacuum; ε_{rw} is the relative permittivity of water; *I* is the ionic strength of the solution; *R* is the gas constant; *T* is the temperature. y^d, the dimensionless potential defined by

$$y^d = F\psi^d / RT \tag{s10}$$

and $$\psi^d = \zeta \qquad \text{(s11)}$$

where ψ^d is generally assimilated to the electrokinetic potential (ζ).

The set of equations s5-s8 can be transformed into

$$\sigma^0 = eN_s \frac{(\left[H^+\right]/K_{a1})\exp(-e\psi^0/kT) - (K_{a2}/\left[H^+\right])\exp(e\psi^0/kT)}{1 + (\left[H^+\right]/K_{a1})\exp(-e\psi^0/kT) + (K_{a2}/\left[H^+\right])\exp(e\psi^0/kT)} \qquad \text{(s12)}$$

A consistent resolution -as achieved by numerical analysis- of equations s1, s2, s9, s11 and s12 allows for a quantitative determination of the double layer parameters that include the various potentials and charges entering the description of the interfacial structure. Further comparison with experimental data (i.e. electrokinetic potentials derived from streaming potential measurements) obtained for a broad range of ionic strengths and pH values enable the evaluation of the quantities pKa$_1$ and pKa$_2$ and N_s. For that purpose, a Least Square Regression (LSR) method was considered.

Modeling In the Case Where There is Specific Ion-Adsorption

Ions of the background electrolyte, which are not primarily charge-determining for a particular type of surface, may be specifically adsorbed onto the surface sites. The non-electrostatic forces involved in this process result in shifts of the point of zero charge and the IEP. For such a reversible interface, the amount of specifically adsorbed ions is, for a given concentration and affinity of these ions, determined by the solution parameter pH. In our experiment, the influence of specific ion adsorption is taken into account by formulating the appropriate equilibrium equations for phosphate groups.

In the low pH range, $SiOH_2^+$ are expected to be the predominant species present at the surface. The surface concentrations of $-SiOH$ and $-SiO^-$ increase upon increasing the pH

value. In the analysis, we considered adsorption of ions onto oppositely charged surface sites, which constitutes the most favorable situation from an energetic point of view. As revealed by electrokinetic experiments performed in NaCl solutions, Na^+ and Cl^- may be considered as indifferent ions. Considering the neutral and negatively charged ions in the phosphate buffer solution, the adsorbability sequence for the various ions present in phosphate solutions onto oxide like surfaces is for low to intermediate pH values as follows $H_3PO_4 \langle\langle H_2PO_4^- \langle\langle HPO_4^{2-3}$. The binding of the pertaining anions onto PDMS surface are expressed by Equations 5-6 in section 3.7. The binding process equilibrium constants are K_x and K_y. It is noted that the respective bulk concentrations of the various relevant phosphate ions were evaluated according to classical speciation calculations based on the first two dissociation p*K*a values reported in the literature.[4-5] The charge density at the solid surface can be calculated from the total amount of charged surface groups that is now written:

$$N_s = [SiOH] + [SiOH_2^+] + [SiO^-] + [SiOH_4PO_4] + [-SiOH_2PO_4^{2-}] \quad \text{(s13)}$$

$$\sigma^0 = [-SiOH_2^+] - [SiO^-] - 2[-SiOH_2PO_4^{2-}] \quad \text{(s14)}$$

The charge density at the inner Helmholtz plane σ^β is determined by the total concentration of adsorbed electrolyte ions:

$$\sigma^\beta = [-SiOH_4PO_4] - 2[-SiOH_2PO_4^{2-}] \quad \text{(s15)}$$

Due to the demand of charge neutrality in a stationary equilibrium, all charge densities must compensate each other as expressed by Equation (s1). From these basic equations

the expressions for the concentrations of the different charged groups can be derived as a function of N_s, K_{a1}, K_{a2}, K_x and K_y. The parameters, N_s, K_{a1}, and K_{a2} were obtained from the analysis of the electrokinetic data obtained in NaCl indifferent electrolyte. On the basis of an iterative numerical analysis of equations s1, s2, s4-s6, s9, s11, s13-s15 and subsequent comparison (following a LSR strategy) with experimental data (ζ potentials) at various ionic strengths and pH conditions, we could evaluate the searched quantities K_x and K_y. We add that the values of the different electrical capacitances introduced in the model and chosen for the analysis were C = 100 μF cm^{-2} (used for the case where no specific adsorption takes place), C1 = 120 μF cm^{-2}, and C2 = 20 μF cm^{-2} as used for the case of specifically adsorbing ions.[3] The (assumed) constancy of these is certainly an abstraction from reality in view of the variation of the silanol distributions (or equivalently of the local balance between hydrophobic and hydrophilic silanol patches) with UV/Ozone treatment time. However, for the lack of better and for the sake of simplicity, we considered oxide-type capacitances as commonly reported in the literature.[1, 3] For that reason, the analysis of the data should certainly be considered at a semi-quantitative level but it has however the merit to reproduce the experimentally observed PDMS surface features, particularly the IEP shifts when varying the phosphate concentration in solution and/or the treatment time and the increase of the surface site concentration with increasing UV/Ozone time exposure. Those features are qualitatively in line with the independent AFM analysis.

References

1. Lyklema, J. *Fundamentals of interface and colloid science Vol. II.* Elsevier Academic Press, **2005**.

2. Duval, J.; Lyklema, J.; Kleijn J.M.; van Leeuwen, H.P. *Langmuir* **2001**, *17*, 7573.
3. Duval, J.; Kleijn, J.M.; Lyklema, J.; van Leeuwen, H.P. *J. Electroanal. Chemistry* **2002**, *532*, 337.
4. Ong, S.W.; Zhao, X.L.; Eisenthal, K.B. *Chem. Phys. Lett.* **1992**, *191*, 327.
5. Wang, B.; Abdulali-Kanji, Z.; Dodwell, E.; Horton, J.H.; Oleschuk, R.D. *Electrophoresis* **2003**, *24*, 1442.